INSTITUTE OF PHYSICS PUBLISHING JOURNAL OF PHYSICS B: ATOMIC, MOLECULAR AND OPTICAL PHYSICS

J. Phys. B: At. Mol. Opt. Phys. **34** (2001) 3025–3039 PII: S0953-4075(01)23129-0

Absolute electron-impact ionization cross sections for a range of C_1 to C_5 chlorocarbons

James E Hudson, Claire Vallance[1], Mark Bart, and Peter W Harland

Department of Chemistry, University of Canterbury, Private Bag 4800, Christchurch, New Zealand

E-mail: p.harland@chem.canterbury.ac.nz

Received 20 March 2001, in final form 10 May 2001
Published 18 July 2001
Online at stacks.iop.org/JPhysB/34/3025

Abstract

Absolute total electron-impact ionization cross sections from threshold to 220 eV are reported for the formation of positive ions from a range of chlorocarbons (one to five carbon atoms), including all chlorine-substituted methanes and ethanes. Correlations between the measured ionization cross section, ionization potential and molecular polarizability volume are explored and compared with data for the perfluorocarbons and mixed halocarbons. A C–Cl bond additivity cross section determined previously for mixed halomethanes has been refined to fit the experimental data for the higher chlorocarbons. Maximum cross sections predicted using bond additivity contributions are shown to be in agreement with experiment for a wide range of molecules to better than $\pm 10\%$ accuracy, and in most cases to better than $\pm 5\%$. The experimental data are compared with the predictions of the Deutsch–Märk and binary-encounter Bethe models.

1. Introduction

Electron-impact ionization plays an important role in many areas of chemistry and physics, including mass spectrometry, plasma processes and gas discharges. Accurate ionization cross sections are important for understanding the mechanism of the ionization process, and are also required for modelling applications, ranging from studies of fusion plasmas to investigations into radiation effects in materials science and medicine. Chlorocarbons, such as CH_3Cl, CCl_4 and CCl_3CH_3, are known to exhibit atmospheric photo-dissociation lifetimes of up to 50 yr; they are potent greenhouse gases and also contribute to ozone loss in the stratosphere [1]. C_1 and C_2 chlorocarbons are used in the semiconductor industry for cleaning chemical vapour

[1] Present address: Physical and Theoretical Chemistry Laboratory, Oxford University, South Parks Road, Oxford OX1 3QZ, UK

0953-4075/01/153025+15$30.00

deposition chambers and also have applications as general purpose solvents, as raw materials in the polymer industry and as dry-cleaning agents [2].

A number of absolute ionization cross section measurements have been published for small chlorocarbons, including the chloromethanes, CCl_3CN, CF_2Cl_2 and CF_3Cl [3, 4]. In this paper, measurements are reported for the chlorine-substituted methanes and ethanes (all isomers), selected ethenes and some C_3 to C_5 chlorocarbons.

There have been many attempts to model electron-impact ionization efficiency curves (the dependence of ionization cross section on electron energy). Two of the more successful ones, the semi-empirical additivity model of Deutsch and Märk [5, 6] and the *ab initio* binary-encounter Bethe theory of Kim and Rudd [7–9], have been used to calculate ionization efficiency curves for comparison with the experimental data. In addition to *ab initio* and semi-empirical models, a previously reported correlation [4, 10, 11] between the maximum ionization cross section and molecular electrostatic properties has been refined to accommodate chlorocarbons with more than one carbon and more than one chlorine atom. This empirical model relates the maximum total ionization cross section, $\sigma_{\max}$, to the molecular volume polarizability α and ionization potential (or appearance energy) E_0 according to the following expression:

$$\sigma_{\max} = c' \left(\frac{\alpha}{E_0} \right)^{1/2} \tag{1}$$

where c' is an empirically determined constant.

One of the fundamental concepts inherent in many theoretical investigations of the electron-impact ionization process is the 'additivity rule', first elucidated by Otvos and Stevenson [12] in the 1950s, according to which a molecular ionization cross section can be determined from the sum of the cross sections of individual atoms, or more generally, of atomic orbitals. The rule is based on Bethe's observation [13] that the probability of ionization of an electron in an n, l atomic orbital is approximately proportional to the mean-square radius of the orbital. In a variation on the additivity rule, Bobeldijk *et al* [14] determined a set of bond contributions to the photoionization cross sections of hydrocarbons and oxygen-containing organic molecules. The contributions were determined from experimental and semi-empirical data, and were found to be in agreement with experiment to within around $\pm 20\%$. We have recently determined a similar set of bond contributions for electron-impact ionization cross sections [4]. Simple addition of these bond contributions has been shown to predict cross sections in very close agreement with experiment for a wide range of molecular systems. Bond additivity cross sections can be rationalized in terms of the same additivity concepts that form the basis of the Deutsch–Märk (DM) and binary-encounter Bethe (BEB) models. An empirical relationship, first reported by Lampe *et al* [15], between the maximum ionization cross section and the polarizability volume is also consistent with the additive nature of the polarizability contributions to the overall molecular polarizability [16, 17].

2. Experimental

The ionization cell used for these measurements, a modified version of the condenser plate ion source used by Tate and Smith [11, 18], has been described previously [3]. The ionization cell is housed in a vacuum chamber with a typical background pressure of $\sim 10^{-7}$ Torr. Electrons are emitted from a resistively heated rhenium filament which is biased at a potential that determines the electron energy. A shield held at a negative potential of 2 V with respect to the filament serves to repel the electrons towards a set of three stainless steel electrostatic lens elements which collimate the electron beam and focus it into the cylindrical collision cell. The

walls of the collision cell are coated with colloidal graphite to prevent surface scattering of charged particles, an important consideration since the cell walls also serve as the ion collector. Previous work has shown that this source gives excellent agreement with the cross sections previously reported for the inert gases and small molecules [3]. Non-volatile samples are vacuum distilled and admitted to the collision cell through a heated inlet line (35 °C) *via* a Leybold–Heraeus needle valve, allowing fine control of the flow rate. The sample pressure admitted to the source was always several orders of magnitude lower than the sample vapour pressure at the temperature of the source. The gases enter the cell through a 3 mm inlet drilled in the cell wall. A second 3 mm aperture in the opposite wall connects the cell to an MKS type 627A, 0.05 Torr full-scale Baratron capacitance manometer. The gas sample is assumed to be in thermal equilibrium with the walls of the collision cell, and a thermistor in contact with the outer wall of the cell is used to measure the gas temperature. After traversing the collision cell, the electron beam passes through two further lens elements before collection on a graphite-coated Faraday plate. The ion current from the collision cell wall and the electron current from the Faraday plate are recorded using Keithley Model 486 picoammeters. All compounds were either Analar or at least greater than 99.0% purity.

Absolute electron ionization cross sections, σ_i, are calculated from

$$\frac{I^+}{I^-} = n\sigma_i x \tag{2}$$

where I^+ and I^- are the measured ion and electron currents, n is the number density of the target gas and x is the path length through the collision cell. Any error introduced by using this approximate form of the Beer–Lambert law lies well within the instrumental error limits for the experiment. Assuming ideal gas behaviour, the above expression can be rewritten as

$$\frac{I^+}{I^-} = \frac{P\sigma_i x}{k_B T} \tag{3}$$

where P and T are the pressure and temperature of the target gas and k_B is Boltzmann's constant.

In a typical experiment, the pressure of the sample gas is maintained at around 3×10^{-4} Torr, and the electron current is kept below 100 nA in order to preclude space-charge effects. Typical ion currents are in the range 0.1–1 nA. The picoammeters used to record the electron and ion currents are computer interfaced through an IEEE parallel bus, while the analogue signals from the thermistor and capacitance manometer (after amplification) are passed to the computer through a commercial 14-bit I/O card. The I/O card is also used to program the electron energy using a Spellman Model MS0.3N, 0 to −300 V, computer-controllable power supply. For each point on an ionization efficiency curve, the electron energy is set and the temperature recorded, the ion and electron currents and target gas pressure are then measured as the average over ten 1 s readings. The resulting ionization efficiency curves are highly reproducible from run to run, even for experiments carried out several weeks apart. The weak oscillation in the ionization efficiency curves above 150 eV is most likely to be due to electron beam focusing effects. We have been able to change the location of the maxima and minima by changing the potentials on the electron focus grids, but we have never been able to eliminate them completely. The results reported here are the average of between five and ten repeated determinations for each target gas made over a period of several months. We have previously determined the accuracy of cross sections measured using this instrument to be 4% or better [3].

Table 1. Experimental and calculated (BEB and DM) maximum total ionization cross sections for the chlorocarbons expressed in units of Å^2 (1 Å^2 = 1 × 10^{-20} m^2). The percentage differences between calculated and experimental values are shown in parentheses.

Molecule	σ_{max}(expt)	σ_{max}(BEB)	σ_{max}(DM)
CH_4	4.23	3.26 (−22.9)	5.05 (+19.4)
CH_3Cl	6.69	5.08 (−24.1)	7.45 (+11.4)
CH_2Cl_2	9.34	6.69 (−28.4)	9.93 (+6.3)
$CHCl_3$	12.73	10.70 (−15.9)	12.80 (+0.5)
CCl_4	15.45	9.76 (−36.8)	15.00 (−2.9)
C_2H_4[a]	5.7	5.28 (−7.4)	6.97 (+22.3)
$C_2H_2Cl_2$	14.49	8.23 (−43.2)	11.14 (−23.1)
C_2HCl_3	18.05	9.78 (−45.8)	15.62 (−13.5)
C_2Cl_4	21.74	11.30 (−48.0)	17.33 (−20.3)
C_2H_6[a]	7.2	5.78 (−19.7)	8.68 (+20.6)
C_2H_5Cl	10.60		
$C_2H_4Cl_2$-1, 1	13.80	8.99 (−34.9)	13.52 (−2.0)
$C_2H_4Cl_2$-1, 2	14.23	8.93 (−37.2)	13.57 (−4.6)
$C_2H_3Cl_3$-1, 1, 2	17.13	10.49 (−38.8)	16.02 (−6.5)
$C_2H_3Cl_3$-1, 1, 1	17.25	10.45 (−39.4)	16.09 (−6.7)
$C_2H_2Cl_4$-1, 1, 2, 2	19.66	12.02 (−38.9)	18.53 (−5.7)
$C_2H_2Cl_4$-1, 1, 1, 2	21.24	11.99 (−43.5)	18.55 (−12.7)
C_2HCl_5	23.61	13.51 (−42.8)	21.06 (−10.8)
C_2Cl_6	26.61	15.10 (−43.3)	23.59 (−11.3)
C_3H_8[a]	10.2	8.39 (−17.7)	12.31 (+20.7)
C_3H_7Cl-1	14.10	9.93 (−29.6)	14.72 (+4.4)
C_3H_7Cl-2	14.22	9.85 (−31.2)	14.72 (+2.9)
C_4H_{10}		10.93	15.94
C_4H_9Cl-1	17.40	12.45 (−28.4)	18.35 (+5.5)
C_4H_9Cl-2	17.12	12.32 (−28.0)	18.35 (+7.2)
t-C_4H_9Cl	17.14		
t-$C_5H_{11}Cl$	19.53		

[a] Values taken from [23].

3. Results and model calculations

Experimentally determined absolute maximum total ionization cross sections are presented in table 1, together with the corresponding DM and BEB results and their percentage deviations from experiment. Figures 1–3 show the experimentally measured ionization efficiency curves over the range from threshold to 220 eV for a selection of the molecules studied, compared with the DM and BEB calculations; in each case the maximum in the cross section, σ_{max}, and the corresponding electron energy, E_{max}, are marked. Model calculations were not carried out for t-C_4H_9Cl and t-$C_4H_{11}Cl$ due to the considerable demands of running molecular orbital calculations on molecules of this size.

We have shown previously [3, 4] that the best choice of model for the calculation of ionization efficiency curves depends on the molecule under study. Table 1 and figures 1–3 show that the DM calculations generally overestimate σ_{max} for molecules of lower molar mass and typically underestimate E_{max} by about 10–15 eV. The DM model performs better on σ_{max} for molecules of higher molar mass, although in all cases the model overestimates the attenuation of the cross section as the electron energy increases above E_{max}. The BEB model was found to give reasonably good fits to experimental ionization efficiency

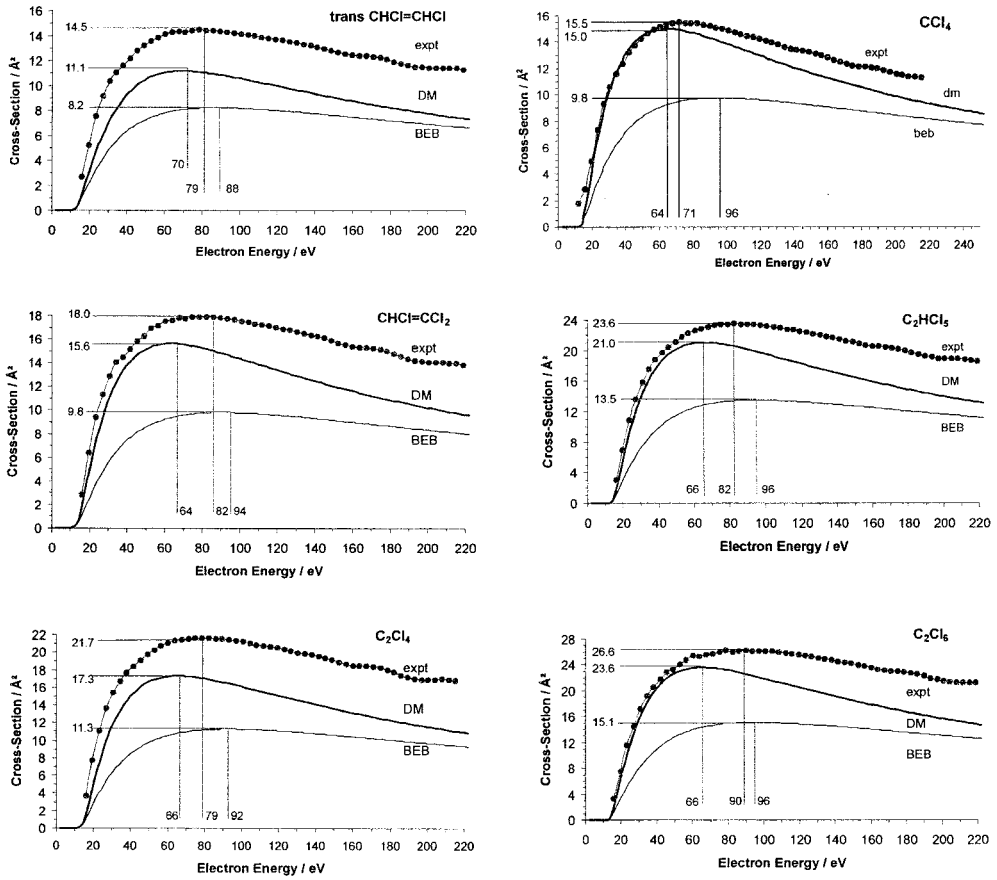

Figure 1. Calculated and experimentally measured total ionization efficiency curves for CCl_4 and the C_2 chlorocarbons: $C_2H_2Cl_2$, C_2HCl_3, C_2Cl_4, C_2HCl_5, C_2Cl_6. The maximum total ionization cross sections σ_{max} and the corresponding electron energies E_{max} are marked on the plots.

curves for the fluoromethanes and the C_1 to C_4 perfluorocarbons [4]; the average deviation from the experimentally determined absolute maximum total ionization cross section for the perfluorocarbons was less than $\pm 5.0\%$. Although the BEB model overestimates E_{max} for the perfluorocarbons by 10–15 eV, the calculated attenuation of cross section with increasing electron energy above E_{max} matches the experimental curves very well. At first glance it would appear that the BEB calculations are not performing well for the chlorocarbons shown in figures 1–3. The value for σ_{max} is underestimated by 30–40% and E_{max} is overestimated by 5–10 eV. This is consistent with the conclusions drawn from measurements of the C_1 chloromethanes, bromomethanes and mixed halomethanes reported previously [4]. The BEB approach does not appear to work well for heavy atoms or where there are several heavy atoms in a hydrocarbon chain. Measurements were made for several sets of isomers, as shown in table 1 and figures 2 and 3.

A closer comparison of the BEB and experimental curves shown in figures 1–3 reveals that the shapes are, in fact, rather well matched over the full electron energy range. In figure 4 the BEB curves for the monochlorocarbons RCl, where R = C_2H_5, n-C_3H_7 and n-C_4H_9, have been multiplied by a factor of 1.4 and compared with the experimental data. The fits are

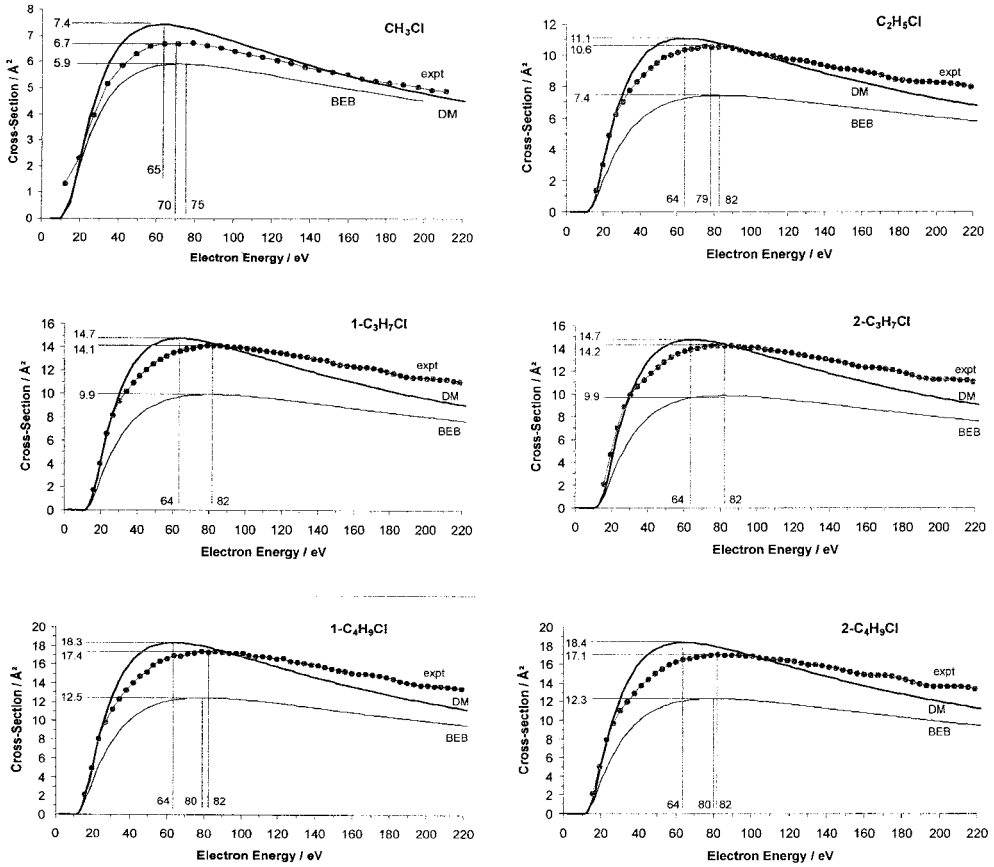

Figure 2. Calculated and experimentally measured total ionization efficiency curves for the C_1 to C_4 monochlorocarbons and their isomers. Values for σ_{max} and E_{max} are marked on the plots.

remarkably good and equivalent to the level of agreement found for the fluorocarbons where a multiplication factor was not required. BEB curves for CH_3Cl, C_2Cl_4 and C_2Cl_6 multiplied by 1.135, 1.9 and 1.7–1.8, respectively, are compared with the experimental results in figure 5. With the exception of the low-electron-energy segment of the ionization efficiency curve for C_2Cl_4, the fits are well within the limitations of experimental uncertainty. These observations apply to all of the hydrocarbons and chlorocarbons shown in table 1 with multiplication factors falling in the range 1.1 for C_2H_4 to 1.9 for C_2Cl_4.

We have considered the possibility that some of the inconsistencies between theory and experiment for molecules containing heavy atoms are due to the level of theory at which the *ab initio* calculations were carried out in the determination of the molecular orbital parameters required by the DM and BEB models. Due to the size of some of the molecules studied, high-level calculations were not practicable in many cases, and for consistency, all calculations were carried out at the HF/6-31G level of theory[2] using the Gaussian 94 molecular orbital code [19]. For selected small molecules, performing molecular orbital calculations using

[2] HF/6–31G denotes Hartree–Fock self-consistent-field molecular orbital calculations carried out with a 6–31G split-valence Gaussian basis set consisting of one contracted basis function containing six Gaussian functions for each core orbital and two contracted basis functions containing three and one Gaussian functions respectively for each valence orbitals

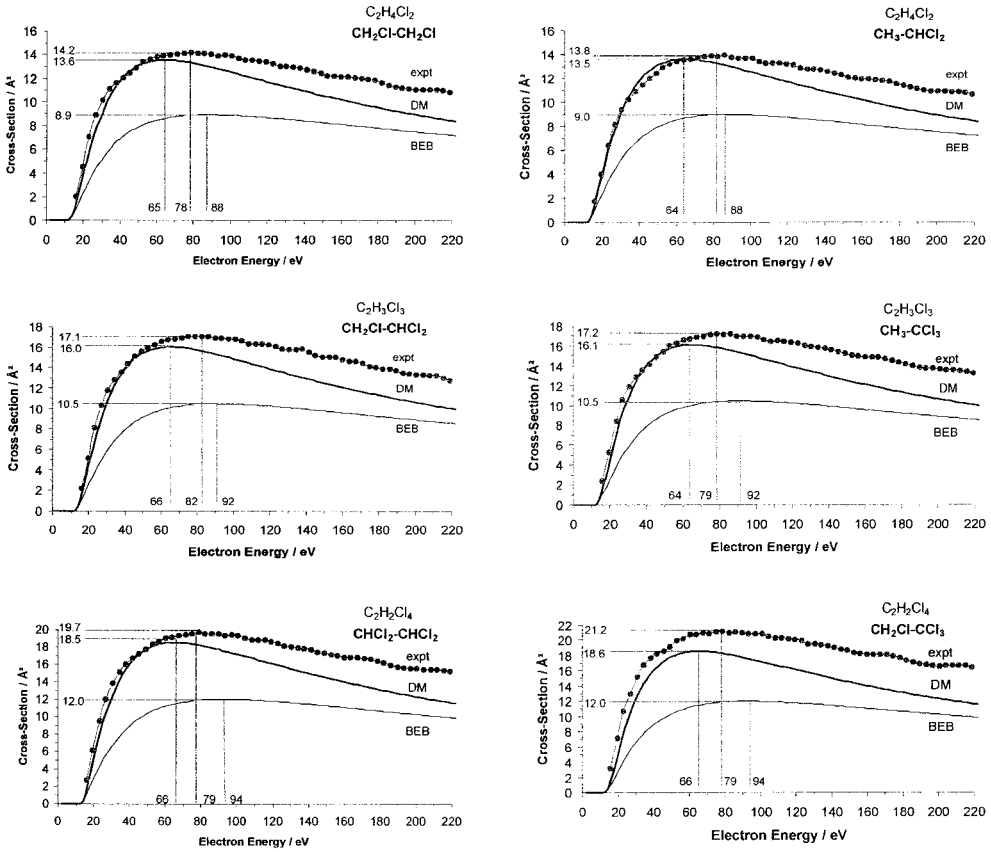

Figure 3. Experimentally measured ionization efficiency curves for all isomeric forms of the C_2 chlorocarbons: $C_2H_4Cl_2$, $C_2H_3Cl_3$, $C_2H_2Cl_4$. Values for σ_{max} and E_{max} are marked on the plots.

larger basis sets and higher levels of theory resulted only in small differences in the calculated cross sections (generally less than 5% over the entire range of electron energies studied), though the effects may become more serious for larger, heavy-atom-containing molecules. If the origin of the observed scaling factors for the BEB calculations is due to deficiencies in the molecular orbital calculations, then it would be expected that the DM calculations should also be affected in some way. However, the trends observed for the DM results in this study agree with those found previously for the fluorocarbons [3, 4] and reported by others [20]. Previously, BEB calculations for the perfluorocarbons at the HF/6-31G level of theory gave very good agreement with experiment. It seems likely that use of a more extensive basis set, in particular the inclusion of polarization functions, may improve the quality of the model cross section calculations. Unfortunately, matters are complicated by an empirical scaling factor introduced by Kim and Rudd for molecular orbitals that are dominated by heavy atom (third row or higher) atomic orbitals [21]. Scaling such orbitals by a factor of the principal quantum number was shown to significantly improve the performance of the BEB model. Identification of such molecular orbitals requires that the basis functions used in the molecular orbital calculations can be assigned to particular atomic orbitals, a procedure whose validity becomes questionable as the basis set is expanded.

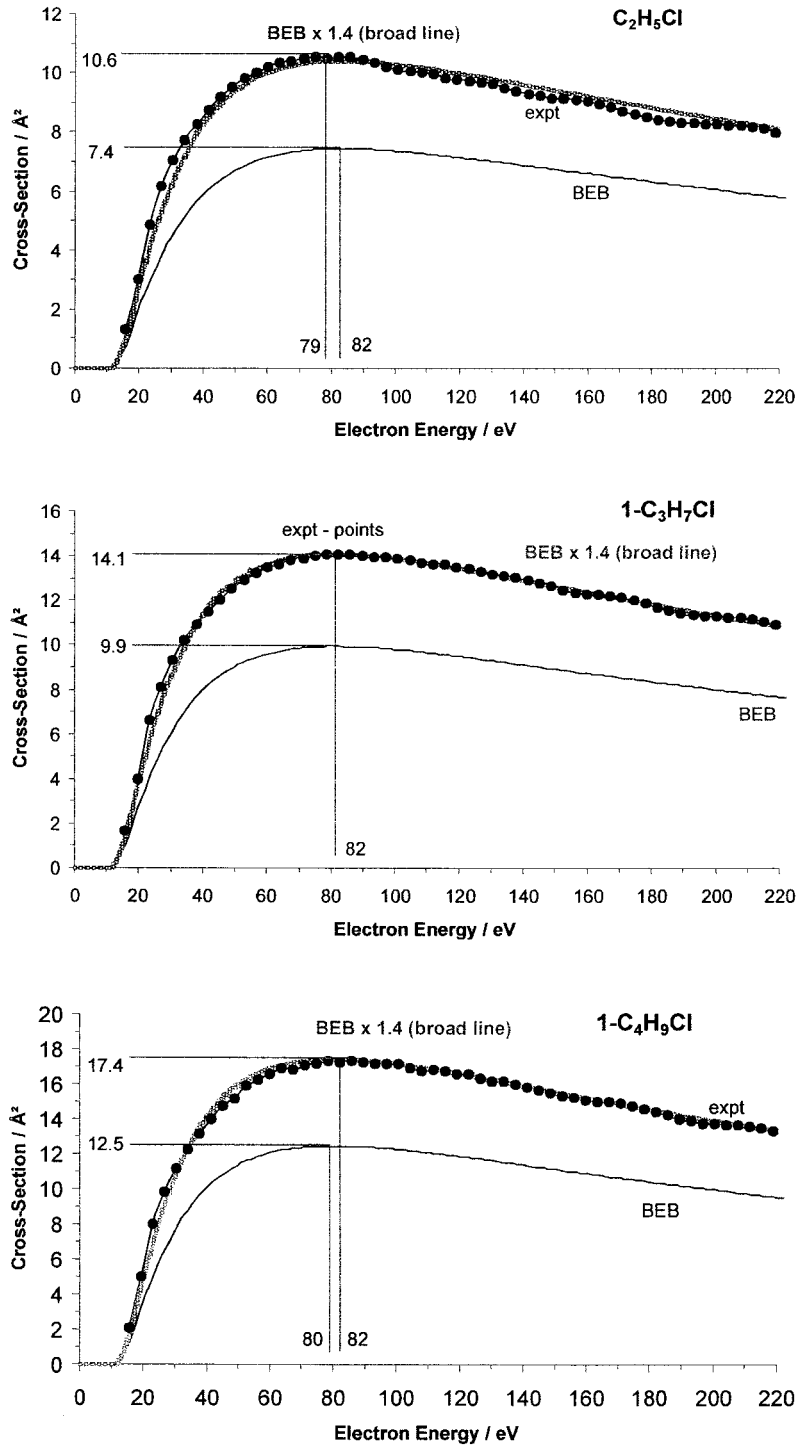

Figure 4. Measured (dots) and BEB (thin full curve) total ionization efficiency curves for the monochlorocarbons C_2H_5Cl, 1-C_3H_7Cl and 1-C_4H_9Cl. BEB curves multiplied by a factor of 1.4 are shown as broad grey lines for each molecule.

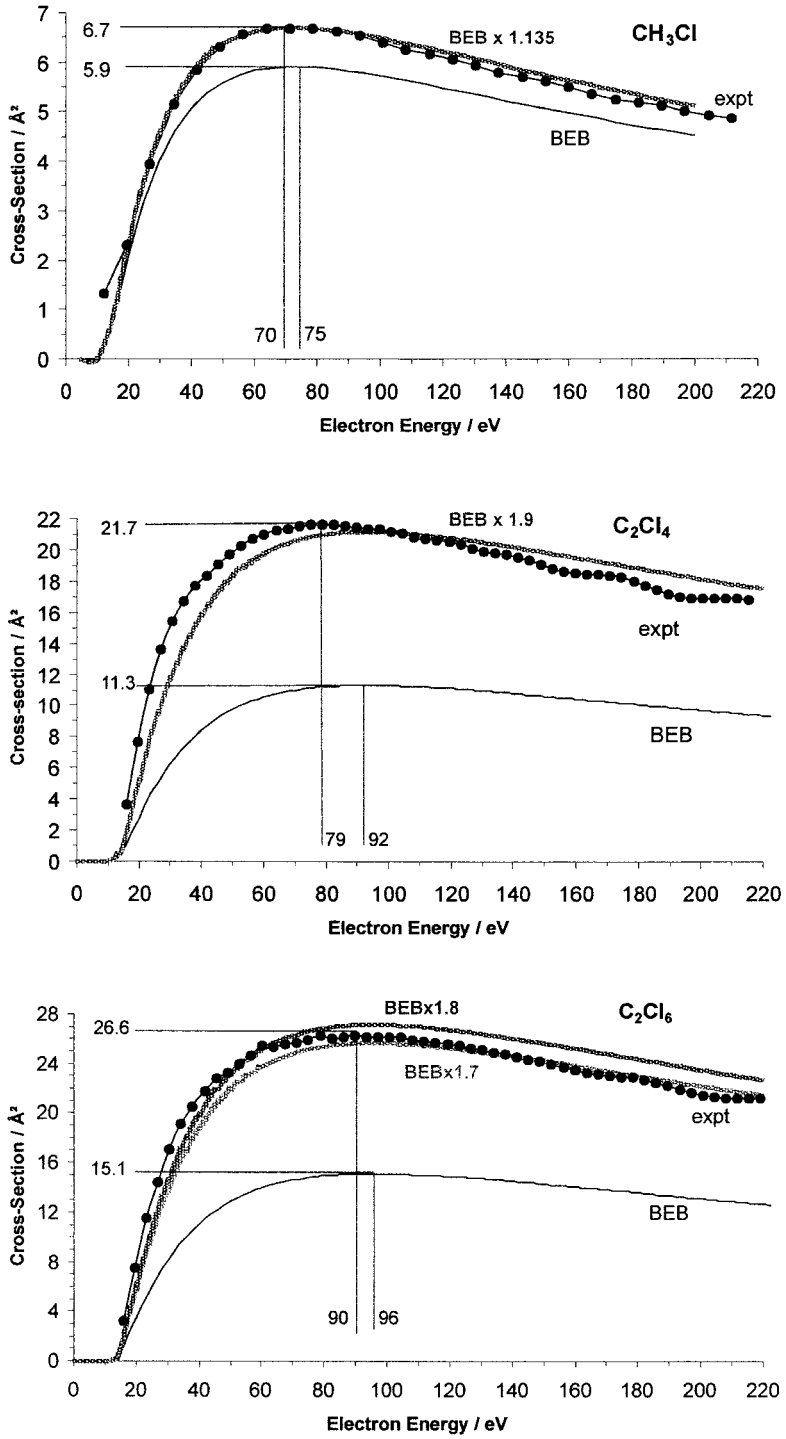

Figure 5. Measured (dots) and BEB (thin full curve) total ionization efficiency curves for CH_3Cl, C_2Cl_4 and C_2Cl_6. BEB curves multiplied by factors of 1.135, 1.9 and 1.7/1.8, respectively, are shown as broad grey lines for each molecule.

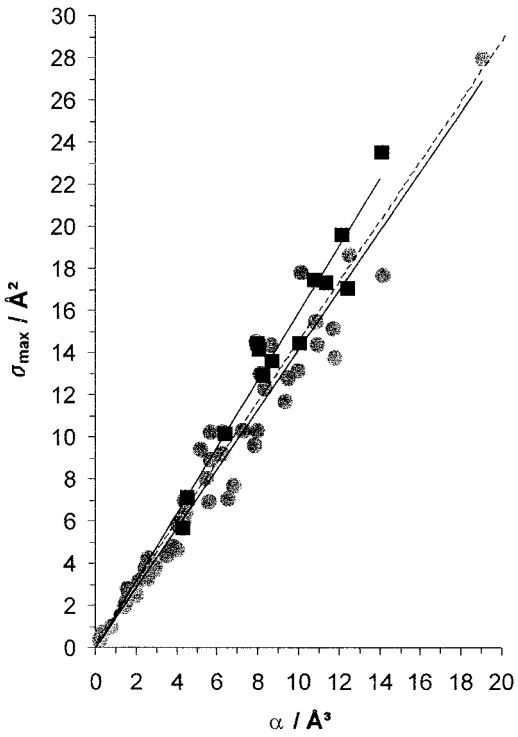

Figure 6. Plot of measured σ_{max} against the molecular polarizability volume: grey circles are the data from [3,4] with a least-squares fitted line, equation (5); full squares are the data from table 1 for the chlorocarbons with a least-squares fitted line, equation (10); the broken line is the least-squares fit to all data, equation (8).

A further consideration is the effect of the dipole oscillator strength on the BEB results. In the absence of experimental or theoretical dipole oscillator strengths for the molecules studied, we have followed the lead of Kim and Rudd [7–9] and set the dipole oscillator constant Q in the BEB equations equal to unity in our calculations. If the true value differs markedly from this approximation, it could lead to a significant discrepancy between measured and calculated cross sections.

4. Correlation with molecular parameters

We have previously reported on relationships between electron-impact ionization cross section and molecular electrostatic parameters [4, 10, 11]. It has been found that linear relationships exist between the maximum cross section σ_{max} and both the molecular polarizability volume α and the quantity $(\alpha/E_0)^{1/2}$, in which E_0 is the ionization potential for production of the molecular ion [22]. Data points for all reported maximum ionization cross sections for atoms and molecules, including our own experimental measurements for small halocarbons and the C_1 to C_4 perfluorocarbons, but excluding the chlorocarbons, are shown as grey circles in figures 6 and 7. Equations (4) and (5) are obtained from least-squares fits to the σ_{max} versus α plot in figure 6. Equation (6) is the least-squares fit to the σ_{max} versus $(\alpha/E_0)^{1/2}$ plot in figure 7.

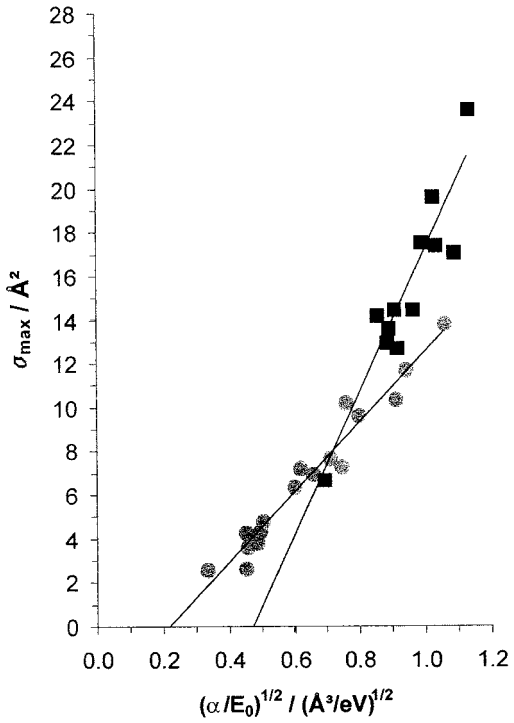

Figure 7. Plot of measured σ_{max} against the square root of the ratio of the molecular polarizability volume to the ionization potential: grey circles are the data from [3, 4] with a least-squares fitted line, equation (6); full squares are the data from table 1 for the chlorocarbons with a least-squares fitted line, equation (11).

Variances, R^2, for the fits are shown in each case.

$$\sigma_{max} = 1.378\alpha + 0.153 \qquad (R^2 = 0.955) \tag{4}$$

$$\sigma_{max} = 1.395\alpha \quad \text{forced through the origin} \qquad (R^2 = 0.955) \tag{5}$$

and

$$\sigma_{max} = 18.13\left(\frac{\alpha}{E_0}\right)^{1/2} - 4.34 \qquad (R^2 = 0.947). \tag{6}$$

In the above expressions, α is in units of $Å^3$ (10^{-24} cm^3) and E_0 is in eV. The full squares in figures 6 and 7 are the data for the chlorocarbons reported here and listed in table 1, and the broken line in figure 6, given by equations (7) and (8), is a least-squares fit through the combined data sets.

$$\sigma_{max} = 1.552\alpha - 0.865 \qquad (R^2 = 0.919) \tag{7}$$

$$\sigma_{max} = 1.453\alpha \quad \text{forced through the origin} \qquad (R^2 = 0.914). \tag{8}$$

Although the expressions have not been greatly changed by the chlorocarbon data, the quality of fit expressed by the variance has decreased significantly. To a large degree, the scatter found in these plots reflects the uncertainties inherent in the polarizability and ionization threshold data. The polarizability and ionization threshold data for the chlorocarbons is incomplete [22], and in some cases it is not readily apparent which of a range of available values is the most

reliable. Despite these limitations, least-squares fits to the chlorocarbon data give an improved fit over the combined data plots, as shown in equations (9) to (11).

$$\sigma_{\max} = 1.570\alpha + 0.198 \qquad (R^2 = 0.935) \tag{9}$$

$$\sigma_{\max} = 1.590\alpha \quad \text{forced through the origin} \qquad (R^2 = 0.935) \tag{10}$$

and

$$\sigma_{\max} = 32.85\left(\frac{\alpha}{E_0}\right)^{1/2} - 15.64 \qquad (R^2 = 0.864). \tag{11}$$

The increased slope noted for the chlorocarbons in figure 6 reflects higher ionization cross sections for a given polarizability, when compared with the inert gases, small molecules, mixed halocarbons and the perfluorocarbons plotted in the same figure. The data for the chlorocarbons in figure 7 reflect this effect, in addition a narrow energy range for the reported ionization potentials of the chlorocarbons (where available) [22] results in an increased slope.

5. Additive bond contributions to the maximum cross section

The experimental maximum ionization cross sections reported in [4] were used to derive a set of additive bond contributions to the maximum molecular ionization cross section, shown in table 2. The maximum total ionization cross section for a molecule is then estimated by simple addition of the contributions from each bond, giving results in close agreement

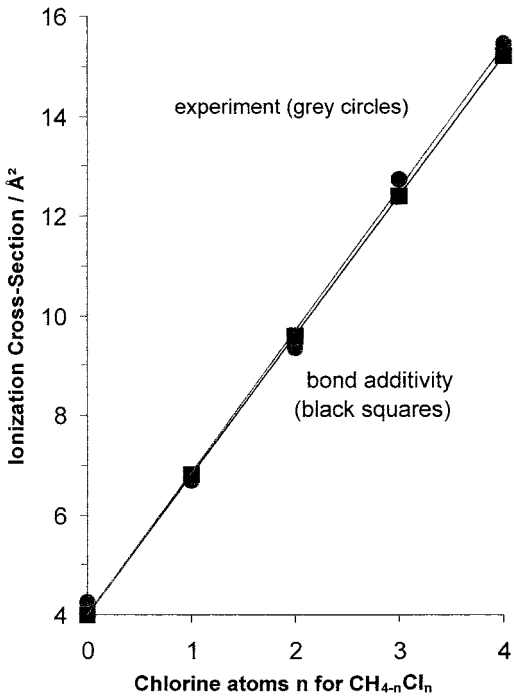

Figure 8. Grey circles show the measured $\sigma_{\max}$ for methane and the chloromethanes as a function of the number of chlorine atoms in the molecule. Black squares are the values for $\sigma_{\max}$ deduced from bond additivity values determined in [4] and reproduced in table 2. The grey and full lines are least-squares fits to the data.

Table 2. Additive bond contributions to the maximum ionization cross section for halomethanes reported in [4] and the modified value for C–Cl from figure 9.

Bond	Cross section component (Å^2)
C–H	1.0
C–F	1.1
C–Cl	3.8 for C = 1
	4.4 for C > 1
C–Br	4.5
C–I	7.3
C–CN	3.0
C–C	1.0
C=C	1.5
C≡C	1.7

with experimentally determined values. As an example, the cross section for CCl_3CN, which cannot be calculated readily using the BEB or DM models, is given by the sum 3(C–Cl) + (C–CN), yielding an estimate of 14.4 Å^2, compared with the measured value of 14.11 Å^2 [4]. Comparison of the maximum electron-impact ionization cross sections determined from bond contributions versus experimental cross section data from [4] shows that all of the experimental cross sections are reproduced to within 10% and most to within 5% (see [4], figure 7). Although the C–H, C–F and C–Cl bond cross sections work well for determining the total cross sections

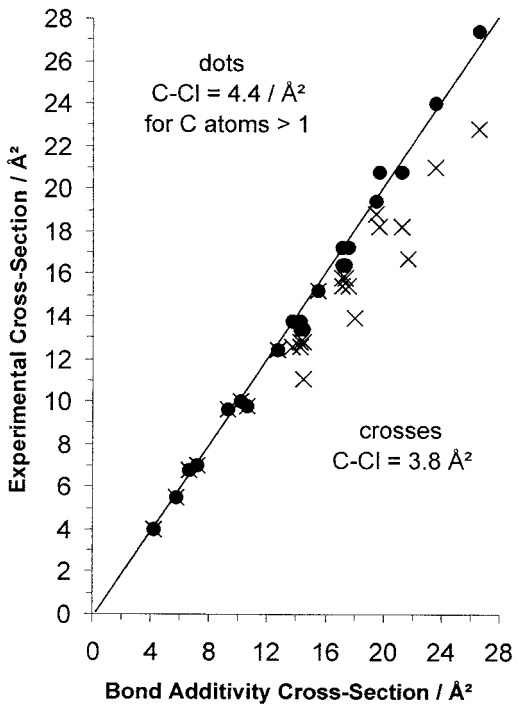

Figure 9. Crosses show the measured σ_{max} for the chlorocarbons listed in table 1 plotted against the values determined from the bond additivity values in table 2 using the value of C–Cl = 3.8 Å^2. Black circles show σ_{max} deduced using C–Cl = 4.4 Å^2 when C > 1.

for a wide range of hydrocarbons, perfluorocarbons and the chlorinated methanes, the C–Cl value determined using the chlorinated methanes results in an underestimation of the total cross section when applied to the higher chlorinated hydrocarbons. This is reflected in figure 7. Figure 8 shows the measured maximum ionization cross section plotted against the number of chlorine atoms in chlorinated methane. The value of 3.8 $Å^2$ for the C–Cl bond contribution to the ionization cross section of the chloromethanes shown in table 2 is obtained from the linear relationship evident in the plot between the cross section and the number of chlorine atoms. Figure 9 shows (a) a plot of the measured chlorocarbon σ_{max} versus the bond additivity values using C–Cl = 3.8 $Å^2$ (crosses) and (b) a value of C–Cl = 3.8 $Å^2$ for the substituted methanes and 4.4 $Å^2$ for molecules with more than one carbon atom (full circles). Agreement between experiment and the modified bond additivity values lies within ±5%.

6. Conclusion

Electron-impact ionization efficiency curves have been measured from threshold to 220 eV for chlorocarbons containing between one and five carbon atoms, and the results compared with calculations using the DM and BEB models.

Though the BEB model performs extremely well at reproducing the general shape of the ionization efficiency curve, the absolute value of the cross section is severely underestimated for the chlorocarbon series. In the past, the BEB model has been used successfully to predict the ionization efficiency curves for a wide range of molecules, including a series of fluorocarbons closely related in structure to the chlorocarbons reported here [4]. The breakdown of the model for the chlorocarbons is therefore somewhat surprising, and at present we have no clear explanation for the cause of the discrepancy. Possible explanations include shortcomings in the molecular orbital calculations or the approximations made in determining dipole oscillator strengths.

The DM model is generally more successful at predicting the magnitude of the ionization cross section, though the functional form of the ionization efficiency curve is not reproduced well at energies higher than the peak, with the calculated curve falling off too fast at high energies relative to the experimental data. This trend is consistent with the behaviour observed previously in studies of other molecular systems [3, 4, 20].

The present data provide further support for the correlation between the maximum electron-impact ionization cross section and the molecular polarizability noted previously [4, 10]. They have also allowed the determination of empirical 'bond contributions' to the maximum cross section from C–Cl bonds. Bond-additivity cross sections calculated using these values, together with the parameters for other bonds determined in a previous publication [4], are in agreement with experiment to within better than ±10%.

Acknowledgments

PWH should like to acknowledge the Marsden Fund for support of this work through grant 99-UOC-032 PSE.

References

[1] Pyle J A, Solomon S, Wuebbles D and Zvenigorodsky S 1992 Ozone depletion and chlorine loading potentials *Scientific Assessment of Ozone Depletion: 1991* (*World Meteorological Organization Global Ozone Research and Monitoring Project Report* no 25) (Geneva: World Meteorological Organization) ch 6

[2] Gerhartz W (ed) 1986 Chlorinated hydrocarbons *Ullmann's Encyclopeadia of Industrial Chemistry* vol A6 (Weinhein: VCH)
[3] Vallance C, Harris S A, Hudson J E and Harland P W 1997 *J. Phys. B: At. Mol. Opt. Phys.* **30** 2465
[4] Bart M, Harland P W, Hudson J E and Vallance C 2001 *Phys. Chem. Chem. Phys.* **3** 800
[5] Margreiter D, Deutsch H and Märk T D 1990 *Contrib. Plasma Phys.* **30** 487
[6] Margreiter D, Deutsch H and Märk T D 1994 *Int. J. Mass Spectrom. Ion Process.* **139** 127
[7] Kim Y K and Rudd M E 1994 *Phys. Rev.* A **50** 3954
[8] Hwang W, Kim Y K and Rudd M E 1996 *J. Chem. Phys.* **104** 2956
[9] Kim Y K, Hwang W, Weinberger N M, Ali M A and Rudd M E 1997 *J. Chem. Phys.* **106** 1026 See also the BEB database and the references therein at http://physics.nist.gov/PhysRefData/Ionization
[10] Harland P W and Vallance C 1997 *Int. J. Mass Spectrom. Ion Process.* **171** 173
[11] Harland P W and Vallance C 1998 *Advances in Gas-Phase Ion Chemistry* vol 3, ed N G Adams and L M Babcock (London: JAI)
[12] Otvos J W and Stevenson D P 1956 *J. Am. Chem. Soc.* **78** 546
[13] Bethe H 1930 *Ann. Phys., Lpz.* **5** 325
[14] Bobeldijk M, Van der Zande W J and Kistemaker P G 1994 *Chem. Phys.* **179** 125
[15] Lampe F W, Franklin J L and Field F H 1957 *J. Am. Chem. Soc.* **79** 6129
[16] See for example, Lippincott E R and Stutman J M 1964 *J. Phys. Chem.* **68** 2926
[17] Zitto M E, Caputo M C, Ferraro M B and Lazzeretti P 2001 *J. Chem. Phys.* **114** 4053
[18] Tate J T and Smith P T 1930 *Phys. Rev.* **36** 1293
[19] Frisch M J *et al* 1995 *GAUSSIAN '94* (Revision A.1) (Pittsburgh, PA: Gaussian Inc.)
[20] Tarnovsky V, Deutsch H and Becker K 2000 *J. Phys. B: At. Mol. Opt. Phys.* **32** L573
[21] Kim Y K private communication
[22] Lide D R (ed) 1993–4 *Handbook of Chemistry and Physics* (Boca Raton, FL: Chemical Rubber Company) 74th edn
http://webbook.nist.gov/
[23] Rapp D and Englander-Golden P 1965 *J. Chem. Phys.* **43** 1464